X-ray absorption spectroscopy of biological photolysis products: kilohertz photolysis and soft X-ray applications

Hongxin Wang[a,b,*], Gang Peng[a], Stephen P. Cramer[a,b]

[a] *Department of Applied Science, University of California, Davis, CA 95616, USA*
[b] *Lawrence Berkeley National Laboratory, Berkeley, CA 94720, USA*

Abstract

In this study, we report the first kilohertz laser photolysis of carbonmonoxy myoglobin (MbCO), studied by hard X-ray absorption spectroscopy (XAS, iron K-edge at ∼7 keV). In addition, traditional frozen photolysis of MbCO has also been evaluated, alternatively, with soft X-ray absorption spectroscopy (iron L-edge at <1 keV). Changes in the K absorption edge position, the pre-K 1s–3d feature and the K-edge XANES spectra have been clearly observed following the photodissociation of MbCO, which shows the structural/electronic changes in between MbCO and its photolysis product Mb*CO, and demonstrates the advanced capacities of our apparatus in monitoring and/or characterizing biological photolysis products. On the other hand, the iron L-edge XAS have shown clearer differences (than K-edge XAS) on the electronic information between the bound MbCO and the photolyzed Mb*CO. The results from these two approaches have been compared and discussed. Practical issues related to the use of kilohertz laser with biological samples, and with synchrotron radiation beamlines, have also been discussed.
© 2004 Elsevier B.V. All rights reserved.

Keywords: Biological photolysis; LFIR; Hard X-ray/soft X-ray measurements

1. Introduction

Photochemically produced biological intermediates were first characterized with X-ray absorption spectroscopy (XAS) in 1984, when Mills et al. [1–4] carried out a pioneer experiment of laser photolysis and XAS probe on flowing solution carbonmonoxy myoglobin complex (MbCO). Their experiment had an extremely low data acquisition efficiency ($\Delta t/T$, as illustrated, in principle, in Fig. 1a) and signal-to-noise (S/N) ratio due to the use of a 20 Hz laser. In their experiments [1–4], over 100 scans were needed in order to obtain a satisfactory XAS spectrum and few spectral details were obtained except an iron K-edge shift of −3 eV upon the laser photolysis. Later on, several studies on biological and inorganic samples [5–9] from time-resolved flowing solution experiments to frozen sample photolysis, from hard X-ray probes to soft X-ray absorption measurements, were reported. However, low repetition lasers still limited the data acquisition efficiency in pulsed experiments while continuous wave (cw) laser has much weaker photolysis power than the pulsed laser photolysis.

In 2001, Jennings et al. [10] reported their development of a kilohertz laser pump and X-ray probe (LPXP) experiment. Their experiment showed an optimized instrumental time-resolution of 14 ns. However, no particular sample application was examined in their experiment and no kilohertz photolysis experiment on a biological or a dilute (e.g. <0.5 wt.%) sample has been reported. In a biological sample measurement, several issues become critical although they seem not so important for instrumental development and/or for materials science studies. First, it is necessary to improve data acquisition efficiency $\Delta t/T$, where T is the period of excitation laser pulses and Δt is the probe time width. For a

* Corresponding author. Tel.: +1 510 486 7319; fax: +1 510 486 5664.
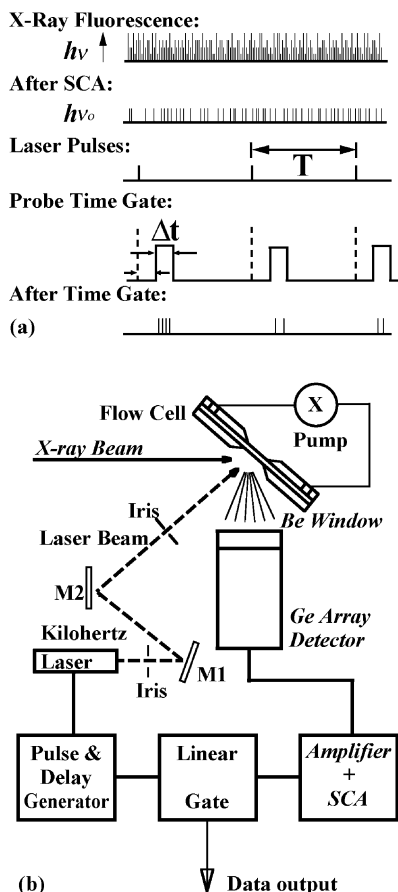*E-mail address:* hongxin@popper.lbl.gov (H. Wang).

Fig. 1. (a) A diagram of data acquisition process and time sequence for a typical laser photolysis/X-ray absorption spectroscopy probe. Time gated X-ray fluorescence signals has a data acquisition efficiency of $\Delta t/T$ where T is the period of laser pulses and Δt is the selected time-window width. (b) The experimental setup for the kilohertz photolysis/XAS probe experiment used in this study. The MbCO solution was photolyzed at 527 nm with a Q-switched kilohertz Nd:YLF laser. Data acquisition was synchronized with laser pulses by a pulse and delay generator and an electronic linear gate.

dilute sample, the time-resolution is often limited by how efficient you can measure the sample, not by instrumental resolution limits. When the signal-to-noise ratio is too poor, you have to select a compromised Δt to improve the data acquisition. In addition, radiation damage is closely related with any biological XAS measurements, let alone the kilohertz photolysis/XAS experiments. The conflict between the need of longer data acquisition time and the concern of radiation damage makes biological samples harder to handle under high flux X-ray/laser irradiation.

Myoglobin is one of the well-characterized metalloproteins. Diatomic O_2, NO and CO can bond to/dissociate from the ferrous iron inside myoglobin, upon which the heme iron undergoes both structural and electronic changes [2,8]. For the past 40 years, photoreactions coupled with different probe techniques including X-ray absorption spectroscopy [1–6] and X-ray crystallography [8] have been used to examine the ligand-binding and ligand-dissociation natures of this heme-protein. A low-temperature crystallographic study in 1994

even revealed the geometric structure of the photodissociation intermediate state Mb*CO [8]. Therefore MbCO is an ideal system for testing the development of new instruments. Besides, the interest in photolyzed Mb*CO is still going on [11,12].

In this study, we report the first kilohertz laser photolysis of carbonmonoxy myoglobin (MbCO), studied by hard X-ray absorption spectroscopy (XAS, iron K-edge at ∼7 keV). In addition, traditional frozen photolysis of MbCO is also evaluated, alternatively, with soft X-ray absorption spectroscopy (iron L-edge at <1 keV). Changes in the K absorption edge position, the pre-K 1s–3d feature, and the K-edge XANES spectra are all clearly observed following the photodissociation of MbCO, which shows the structural and electronic changes in between MbCO and its photolysis product Mb*CO. On the other hand, the iron L-edge XAS show clearer differences (than K-edge XAS) on the electronic information between the bound MbCO and the photolyzed Mb*CO. The results from these new approaches are compared.

2. Experimental

The deoxy myoglobin (deoxy Mb) and carbonmonoxy myoglobin (MbCO) solution of 1 mM were prepared from horse heart myoglobin (Sigma, 99.5%) according to a published procedure [1–4]. An aluminum flow cell with a 2 mm × 2 mm double windows was used to flow the MbCO solution during the laser photolysis/XAS measurement, in the first part of this study, to prevent MbCO from degradation by laser firings and X-ray radiation. MbCO was circulated by a fast peristaltic pump at a speed of 2.0 cc/s, which allowed the irradiated portion of sample be completely renewed after each laser shot. We noted that about 20% of the ground state molecules were flowed into the probe area in between each XAS measurement (in the first 200 μs following each laser pulse). There could be a 0.06 °C increase per laser pulse assuming photons absorbed from a laser pulse were all converted to heat, but no heat accumulation was observed. This is due to the fast heat dispersion via a big copper base attached to the aluminum flow cell and cooled with a chiller maintained at ∼5 °C. From the XAS spectra, we did not observe spectral changes from scan to scan. The whole solution sample was still changed every two scans to avoid radiation damage.

The MbCO solution was photolyzed with 527 nm green light from of a Q-switched and internally frequency-doubled kilohertz Nd:YLF laser (Photonics Industries, GM-30). To save the limited hutch space, only the laser head was placed inside the beamline hutch while the power supply and other electronics were kept outside the hutch (see Fig. 1b). For this purpose, the high voltage cable and other control cables between the power supply unit and the laser head unit had to be extended to 30 ft. Although speculated, no pulse splitting or distortion was found in the photolysis laser pulses in this instance for operation <3 kHz. For op-

eration >3 kHz, the laser pulses start to broaden and distort from a Gaussian profile. Considering both the laser power output and the laser pulse integrity, the best experimental condition was found at 1–3 kHz repetition rate. The 527 nm laser beam was directed and dispersed onto the sample via two adjustable high reflection UV–vis mirrors (M1 and M2).

Although up to 20 mJ/pulse laser output is available from GM-30, excessive photolysis power was restricted in order to reduce the possible radiation damage to the MbCO. The 1 mM (c) and 1 mm (x) thick solution in the 2 mm × 2 mm probing area has 2.5×10^{15} MbCO molecules. The MbCO absorption coefficient is 2×10^4 M cm^{-1} (m_a) [1] which corresponds to an estimated optical density of $m_a c x = 1$, or 90% in optical absorption when one-to-one photon bombardment is considered. Assuming unit photodissociation yield for MbCO [13] about 3×10^{15} (2.5 mJ/pulse) photons will be enough for a >90% photolysis. In this experiment, an attenuated laser power of 5 mJ/pulse (twice as much as the theoretically required value) was used to photolyze the MbCO solution when the laser was operated at 1 kHz. Higher laser power is necessary when a higher repetition rate is used.

The XAS measurements were performed at the Stanford Synchrotron Radiation Laboratory (SSRL), beamline 4-2, with an X-ray resolution of 2.0 eV and a beam size of 3 mm × 4 mm. A 13-element germanium array detector (Canberra, GUL00505) was used to collect X-ray fluorescence and a beryllium window was used to keep the detector under high vacuum and to block the strong laser scattering. Analog signals from the detector (F) [14,15] were amplified (Canberra, 2026), windowed at the Fe Kα energy (SCA, Tennelec, TC452), and sent to scalers and a control computer for data processing and spectral display. The beam intensity (I_0) was monitored with an ion chamber in front of the flowing cell. The fluorescence signal was normalized to I_0 to obtain an XAS spectrum while the incident X-ray beam was scanned over the energy range of 7100–7250 eV. The integration time for the XAS measurements was 3 s/point and the final spectrum was the sum of four such scans. The spectra were calibrated by taking XAS of a standard iron film (K-edge at 7112 eV).

For measuring the Mb*CO, the data acquisition was time discriminated by an electronic linear gate (Philips Scientific, 7450) in between each SCA and each scaler. The overall apparatus is similar to those described previously [1–6] and combined with a typical laser pump-probe measurement [16–19]. The SCA windowed X-ray fluorescence signals were time gated at the given time gap (Δt) for every photolysis cycle (T). TTL pulses from a pulse and delay generator (EG&G, 9650) were used to trigger the kilohertz Nd:YLF laser and to synchronize the data acquisition with the laser photolysis via the linear gate. As shown in Fig. 1a, the X-ray source (average burst interval <200 ns) can be treated as a cw source in comparison with the photolysis laser source (interval = 1 ms at 1 kHz). The data acquisition time gap (Δt) in this experiment was set at 100 μs, with a time delay of 100–800 μs in respect to the laser pulses.

Soft X-ray spectra were measured at the SSRL, beamline 10-1 and 8-2, using a setup similar to those reported previously for other non-photolysis biological applications [20,21]. In brief, windowless operation was used between the storage ring, sample and a 13-element germanium detector, under a vacuum of 3×10^{-9} Torr or better. The energy resolution was at about 0.4 eV and the beam spot size was ~2 mm × 2 mm. Regular data acquisition electronics (amplifiers, SCAs and scalers) were used, and no linear gate/pulse generator was needed. The SCA resolved iron fluorescence signal (F) was normalized to the incident X-ray flux (I_0) measured by electron yield to obtain an XAS spectrum while the X-ray source was scanned over the energy region of 700–740 eV. The spectra were calibrated using Fe$_2$O$_3$ with an L$_3$ peak at 709 eV.

Soft X-ray measurements for our myoglobin samples were performed by the following sequence: (1) let deoxy Mb and MbCO solution dry on a sample holder, to form partially dehydrated thin films, and load them into the measurement chamber with a loadlock; (2) measure the iron L-edge XAS of deoxy Mb and MbCO films; (3) photolyze MbCO by irradiating the film with a cw He–Ne laser (MWK, 633 nm, 10 mW) for about half an hour; (4) measure the iron L-edge XAS of the photolysis product Mb*CO. Liquid helium (LHe) cryogenic temperature (<10 K) was applied, with a LHe flow cryostat, to preserve the Mb*CO from recombining into MbCO [22,23] and to prevent the biological samples from radiation damage in general. An integration time of 5 s/point was used during data acquisition and the final spectra were the sum of 20 scans. Every five scans, the sample position was changed and the above procedure was repeated to avoid possible radiation damage. On comparing the data from different scans, we observed no radiation damage to the samples.

3. Results and discussion

The iron K absorption edges of MbCO prior to (solid line) and following (dashed line) the 527 nm laser photodissociation are shown as in Fig. 2. The K absorption edge for the photolysis product Mb*CO was found to shift −2.7 eV in comparison with that for MbCO, which is consistent with the previous results [1–4]. The measurements were also performed for the photolysis product Mb*CO at different time delays following the kilohertz laser photolysis. Less K absorption edge shift in between Mb*CO and MbCO was observed for a longer time delay (Fig. 2, top right inset), suggesting a recombinable Mb* + CO [22,23]. This result is consistent with previous findings [22,23] as well as with the crystallographic data that shows the unligated CO is still inside the myoglobin molecule [8,24]. The edge shift versus the delay more or less follows a decaying exponential curve (not shown), as expected. This measurement also demonstrates the feasibility of using different detector elements to detect
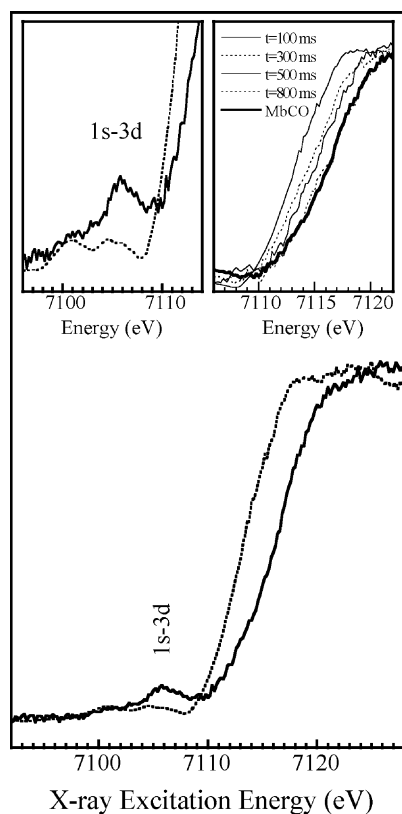
Fig. 2. The iron K absorption edge prior to (solid line) and following (dashed line) the 1 kHz laser photolysis of MbCO at 527 nm. The time delay between the photolysis and the XAS data collection was 100 μs with a time gate of 100 μs in width. The top left inset shows an expanded view of the 1s–3d feature with the MbCO spectrum being arbitrarily shifted upwards for better viewing. The top right inset shows the iron K-edge spectra in the edge region of MbCO (the thick solid line at the right most) and Mb*CO with different time delays, at 100 μs (thin solid line), 300 μs (thin dashed line), 500 μs (thin solid line) and 800 μs (thin dashed line), respectively.

the iron Kα fluorescence with different probe delay at the same time.

More important, clear spectral profiles and dramatic changes have been observed in the pre-K 1s–3d region (see Fig. 2, top left inset). The 1s–3d exhibits a clear and single transition for MbCO and a much weaker double peak for Mb*CO. One explanation suggests that 3d + 4p orbital mixing may exist in the CO complex to enhance the 1s–3d transition, but at least partially removed in Mb*CO. A small amount of the dipole allowed 1s–4p transition will introduce appreciable intensity to the dipole-forbidden 1s–3d transition. Also MbCO has a single transition intensity due to its low spin configuration whereas Mb*CO has a dispersed transition intensity due to the high spin configuration [25]. By fitting the 1s–3d multiplet, it is even possible to understand detailed orbital symmetry and/or electronic information out of a well-resolved 1s–3d spectrum [26]. Being able to observe clear profiles with four XAS scans well demonstrates the advanced capacity of our apparatus in comparison with other previous biological studies [1–6].

We also observed significant differences between MbCO and Mb*CO in the XANES region, as shown in Fig. 3. In studying myoglobin, the XAS in this region can be used to retrieve information about the ligand field and the induced "heme distortion". Chance and Miller correlated a ligand field indication ratio (LFIR = A/B, see Fig. 3 lower inset), to the distance between the iron atom and the heme plane inside myoglobin (M-Ct) [27]. According to their correlation, the least-square linear fit is LFIR = 2.3M-Ct + 0.66. Using this procedure, the LFIR (and M-Ct) were found as A/B = 0.7 (M-Ct = 0.02 Å) for MbCO and A/B = 1.2 (M-Ct = 2.4 Å) for Mb*CO, respectively. These values are consistent with the crystallographic data (MbCO: 0.05 Å; Mb*CO: 2.7 Å) [8].

Kilohertz laser photolysis versus 20 Hz laser photolysis improved the probe efficiency by a factor of 50. Multiple-element germanium detector and advanced electronics provided another 3–5 times better S/N. In total, there is over 200 times better statistics for a time-resolved measurement using our apparatus than using the earlier generations of biological photolysis apparatus [1–6]. With this good efficiency, our apparatus enables us to obtain a good spectrum with only 4 scans rather than 100 scans [1–4] and to record a spectrum with a finer energy step (e.g. 0.2 eV) for more spectral details. Also with this good efficiency, it is even feasible to measure photolysis with better time resolution while achieving the same S/N as previous biological photolysis. As we mentioned in the introduction, the real time resolution in a biological mea-
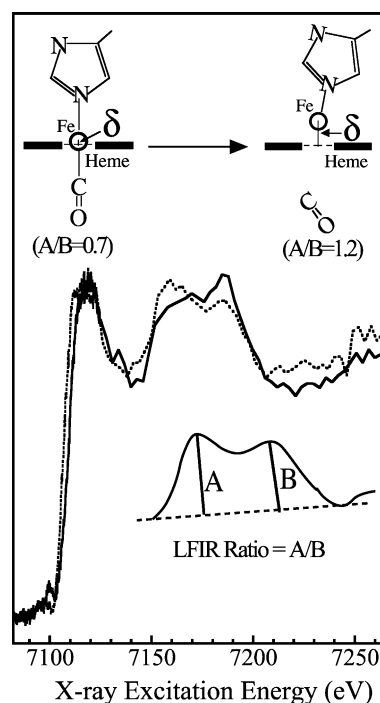

Fig. 3. The iron K-edge XANES spectra (up to 7250 eV) prior to (solid line) and following (dashed line) the 1 kHz laser photolysis of MbCO at 527 nm. The time delay between the photolysis and the XAS data collection was 100 μs with a time gate of 100 μs in width. The top inset shows the illustrated MbCO and Mb*CO structures while the bottom inset shows the ligand field indication ratio LFIR (see text for details).

surement is usually not determined by the instrumental resolution (laser 100 ns/X-ray 2 ns), but determined by how small you can set Δt and still be able to get a good enough S/N. If we assume Mills' experiment [1–4] had a time resolution of $\Delta t = 100\,\mu s$, then $\Delta t < 1\,\mu s$ can be used in our apparatus with the same S/N and data acquisition time.

The soft X-ray iron L-edge absorption (XAS) spectra of MbCO (upper, solid line), deoxy Mb (lower, solid line) and Mb*CO (upper and lower, dashed lines) are shown as in Fig. 4. The L-edge XAS exhibits much richer multiplet features because of the strong interaction of a 2p core hole with 3d electrons. The 3d electrons can be arranged into two common configurations, a low spin configuration where all the possible electrons are paired (with $S = 0$ or 1/2), and a high spin configuration where all the possible electrons are unpaired (with $S > 1/2$). In general, a 3d metal center with a low spin electronic configuration will have single absorption peaks in the L_3 and L_2 regions. The $L_3/(L_2 + L_3)$ intensity branching ratio will be low. On the other hand, a 3d metal with a high spin configuration will have a structured multiplet in both L_3 and L_2 regions, with a higher branching ratio. The low spin/high spin XAS spectra can better be identified with multiplet calculation and/or XAS comparison with known model compounds – both are well studied and well published [28–32].
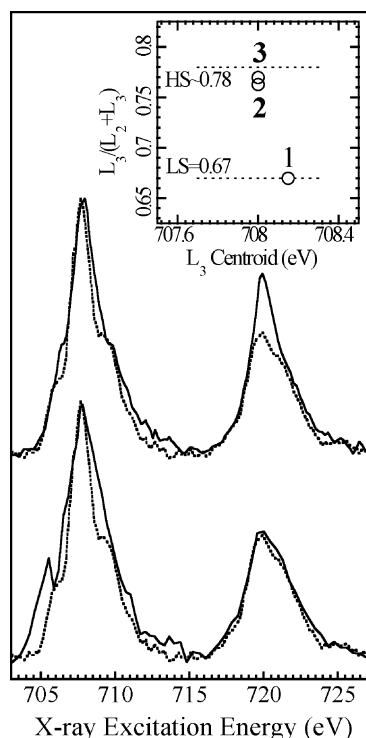

Fig. 4. The iron L-edge XAS for MbCO (solid line) vs. the photolyzed Mb*CO (dashed line) (upper spectra), and the iron L-edge XAS for deoxy Mb (solid line) vs. Mb*CO (dashed line) (lower spectra). The top right inset is the branching ratio correlation diagram. The two dashed lines are the theoretical branching ratios for high spin and low spin Fe(II) sites, respectively, while the solid round symbols indicate the observed branching ratio values for MbCO (1), deoxy Mb (2) and Mb*CO (3).

From previous studies [1–4] it is known that deoxy Mb, MbCO and Mb*CO all have a ferric iron site (Fe(II) d6), so we only need to discuss Fe(II) here. Our L-edge spectrum for MbCO has relatively structure-less L_3 and L_2 peaks and a low branching ratio, which is consistent with a low spin Fe(II) site (d6, $S = 0$) [33,34]. The spectra for the deoxy Mb and Mb*CO have rich multiplets in L_3 and L_2, with significantly higher branching ratios, indicating high spin (d6, $S = 2$) configurations for them [33,34]. The low → high spin transition form MbCO → Mb*CO, observed in the iron L-edge XAS here, is in agreement with the intensity changes found in the pre-K 1s–3d region. However, L-edge spectra exhibit a much clearer change between MbCO and Mb*CO, than the 1s–3d feature.

As mentioned above, branching ratio of $L_3/(L_2 + L_3)$ is a sensitive indicator for the electronic configuration of the metal centers. These branching ratio values can be calculated theoretically and correlated to the electronic configurations of the probed metal species. For example, a low spin Fe(II) has a theoretical branching ratio of 0.67 while a high spin Fe(II) has a ratio of 0.78 [33,34]. In this study, MbCO, deoxy Mb and Mb*CO have experimental branching ratios (corrected to the fluorescence yield differences [35]) of 0.67, 0.76 and 0.77, respectively, suggesting that the first one has a low spin Fe(II) while the rest two have high spin Fe(II). These values are illustrated as in Fig. 4 (top inset). The two dashed lines are the theoretical branching ratio values for the ideal high spin and low spin Fe(II) sites, respectively, from the published data [33,34]. For some spectra where the "peaks" are broad rather than sharply structured, the multiplet itself may not be obvious in determining the electronic spin states and this branching ratio correlation will play a critical role.

Although there is almost no difference in the iron K-edge XAS [1–4] and not much difference in the branching ratios, deoxy Mb and Mb*CO have significant differences in the iron L-edge multiplet. These subtle spectral differences are consistent with the fact that Mb*CO has a caged and recombinable CO [22,23] while deoxy Mb has no CO at all. The minor structural difference can affect the Fe(II) 3d orbitals, which in turn can be observed with L-edge XAS due to its 2p–3d interaction. Being able to probe this subtle difference well illustrates the sensitivity of the L-edge XAS in probing the detailed 3d electron/orbital information. This sensitivity becomes even more important in monitoring photoreactions because the 3d orbitals are bonding orbitals involved in UV–vis excited transitions, such as d–d and metal ligand charge transfer transitions, and L-edge XAS transitions directly probe the unoccupied 3d orbitals.

As discussed above and illustrated in Fig. 5, a clearer and calculable spectral multiplet and a direct probe of photoreaction involved (3d) orbitals are great advantages for soft X-ray L-edge XAS over hard X-ray K-edge XAS in resolving electronic information in systems with 3d transition metals. However, hard X-ray measurements still have their own advantages. Metal K-edge data provides both electronic and structural information, while L-edge absorption only pro-
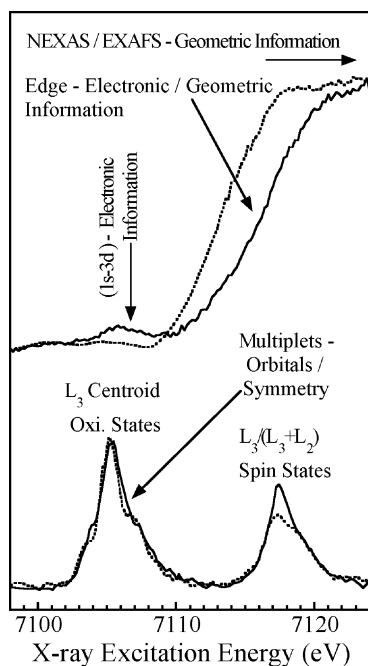
Fig. 5. The iron K-edge spectra prior to (solid line) and following (dashed line) the 1 kHz laser photolysis of MbCO vs. the soft X-ray iron L-edge spectra for MbCO and Mb*CO overlaid in the same K-edge region. It is clear that L-edges provide better electronic information while K-edges have both electronic and structural information.

vides electronic information. In addition, hard X-ray absorption is really bulky-sensitive while soft X-ray only probes the first fraction of a micrometer of the sample surface. Besides, due to the UHV requirement, the soft X-ray experiment cannot be (or at least is very difficult to be) associated with a flowing pump and probe measurement. Therefore, hard X-ray and soft X-ray measurements will be complementary to each other in providing the full information. It will be better to have both.

4. Summary

In this study, the first kilohertz laser photolysis of carbonmonoxy myoglobin (MbCO) was studied by hard X-ray absorption spectroscopy (iron K-edge at ∼7 keV). Our measurement has over 200 times better statistics than earlier generations of biological photolysis/XAS measurements. With this improved efficiency, we are able to measure the spectra faster and to reveal more spectral details in K-edge XAS for MbCO and for the photolyzed Mb*CO. Among them are better features in the 1s–3d region and the LFIR (and the M-Ct distances) obtained from the NEXAS region. In addition, traditional frozen photolysis of MbCO was also evaluated with soft X-ray absorption spectroscopy (iron L-edge at <1 keV). Relative to the K-edge results, the iron L-edge XAS shows clearer differences between the bound MbCO and the photolyzed Mb*CO and shows rich multiplet features which are useful for revealing the details of 3d electronic structure.

The XAS data obtained with these two approaches are in agreement with and complementary to each other, and the comparison of them well illustrates the usefulness of both measurements in studying biological photolysis products.

References

[1] D.M. Mills, Nucl. Instrum. Meth. Phys. Res. A 222 (1984) 159.
[2] D.M. Mills, Phys. Today (USA) 37 (1984) 22–30.
[3] D.M. Mills, A. Lewis, A. Harootunian, J. Huang, B. Smith, Science (USA) 223 (1984) 811–813.
[4] D.M. Mills, V. Pollock, A. Lewis, A. Harootunian, J. Huang, Nucl. Instrum. Meth. Phys. Res. A 222 (1984) 351–354.
[5] A. Clozza, A. Congiu Castellano, S. Della Longa, A. Giovannelli, A. Bianconi, Rev. Sci. Instr. 60 (1989) 2519–2521.
[6] M.R. Chance, M.D. Wirt, E.M. Scheuring, L.M. Miller, A.H. Xie, D.E. Sidelinger, Rev. Sci. Instr. 64 (1993) 2035–2036.
[7] D.J. Thiel, P. Livins, E.A. Stern, A. Lewis, Nature 362 (1993) 40–43.
[8] I. Schlichting, J. Berendzen, G.N. Phillips, R.M. Sweet, Nature 371 (1994) 808–812.
[9] H.X. Wang, G. Peng, L.M. Miller, E.M. Scheuring, S.J. George, M.R. Chance, S.P. Cramer, J. Am. Chem. Soc. 119 (1997) 4921–4928.
[10] G. Jennings, W.J.H. Jager, L.X. Chen, Rev. Sci. Instrum. 73 (2001) 362–368.
[11] J. Vojtechovsky, K. Chu, J. Berendzen, R.M. Sweet, I. Schlichting, Biophys. J. 77 (1999) 2153–2174.
[12] D.E. Sagnella, J.E. Straub, T.A. Jackson, M. Lim, P.A. Anfinrud, Proc. Natl. Acad. Sci. U.S.A. 96 (1999) 14324–14329.
[13] L.M. Miller, M.R. Chance, J. Am. Chem. Soc. 116 (1994) 9662–9669.
[14] M.M. Grush, G. Christou, K. Hamalainen, S.P. Cramer, J. Am. Chem. Soc. 117 (1995) 5895–5896.
[15] J. Chen, J. Christiansen, R.C. Tittsworth, B.J. Hales, S.J. George, D. Coucouvanis, S.P. Cramer, J. Am. Chem. Soc. 115 (1993) 5509–5515.
[16] H.X. Wang, X.R. Chen, B.R. Weiner, Chem. Phys. Lett. 216 (1993) 537–543.
[17] H.X. Wang, X.R. Chen, B.R. Weiner, J. Phys. Chem. 97 (1993) 12260–12268.
[18] X.R. Chen, H.X. Wang, B.R. Weiner, M. Hawley, H.H. Nelson, J. Phys. Chem. 97 (1993) 12269–12274.
[19] M. He, H.X. Wang, B.R. Weiner, Chem. Phys. Lett. 204 (1993) 563–566.
[20] S.P. Cramer, G. Peng, J. Christiansen, J. Chen, J. Vanelp, S.J. George, A.T. Young, J. Electron. Spectrosc. Relat. Phys. 78 (1996) 225–229.

[21] H.X. Wang, C.Y. Ralston, D.S. Patil, R.M. Jones, W. Gu, M. Verhagen, M. Adams, P. Ge, C. Riordan, C.A. Marganian, P. Mascharak, J. Kovacs, C.G. Miller, T.J. Collins, S. Brooker, P.D. Croucher, K. Wang, E.I. Stiefel, S.P. Cramer, J. Am. Chem. Soc. 122 (2000) 10544–10552.

[22] M.R. Chance, S.H. Courtney, M.D. Chavez, M.R. Ondrias, J.M. Friedman, Biochemistry (USA) 29 (1990) 5537–5545.

[23] J.M. Friedman, D.L. Rousseau, M.R. Ondrias, R.A. Stepnoski, Science (USA) 218 (1982) 1244–1246.

[24] T.Y. Teng, V. Srajer, K. Moffat, Nature Struct. Biol. 1 (1994) 701–705.

[25] T.G. Spiro, T.C. Strekas, J. Am. Chem. Soc. (USA) 96 (1974) 338–345.

[26] T.E. Westre, P. Kennepohl, J.G. DeWitt, B. Hedman, K.O. Hodgson, E.I. Solomon, J. Am. Chem. Soc. 119 (1997) 6297–6314.

[27] L.M. Miller, M.R. Chance, Biochemistry (USA) 34 (1995) 10170–10179.

[28] G. van der Laan, I.W. Kirkman, J. Phys. Cond. Matt. 4 (1992) 4189–4204.

[29] F.M.F. de Groot, J.C. Fuggle, B.T. Thole, G.A. Sawatzky, Phys. Rev. B 42 (1990) 5459–5468.

[30] G. Peng, J. Vanelp, H. Jang, L. Que, W.H. Armstrong, S.P. Cramer, J. Am. Chem. Soc. 117 (1995) 2515–2519.

[31] J. Vanelp, S.J. George, J. Chen, G. Peng, C.T. Chen, L.H. Tjeng, G. Meigs, H.J. Lin, Z.H. Zhou, M.W.W. Adams, B.G. Searle, S.P. Cramer, Proc. Natl. Acad. Sci. U.S.A. 90 (1993) 9664–9667.

[32] X. Wang, F. Degroot, S.P. Cramer, J. Electron. Spectrosc. Relat. Phys. 78 (1996) 337–340.

[33] G. van der Laan, Phys. B 158 (1989) 395–397.

[34] C.C. Moulin, P. Rudolf, A.M. Flank, C.T. Chen, J. Chem. Phys. 96 (1992) 6196.

[35] F.M.F. Degroot, M.A. Arrio, P. Sainctavit, C. Cartier, C.T. Chen, Solid State Commun. 92 (1994) 991–995.